Journal of Archaeological Science 101 (2019) 72–88

Contents lists available at ScienceDirect

Journal of Archaeological Science

journal homepage: www.elsevier.com/locate/jas

Scrapping ritual: Iron Age metal recycling at the site of Saruq al-Hadid (U.A.E.)

Ivan Stepanov[a,*], Lloyd Weeks[a], Kristina Franke[a], Thomas Rodemann[b], Filomena Salvemini[c], Charlotte Cable[a], Yaaqoub Al Ali[d], Mansour Boraik Radwan[d], Hassan Zein[d], Peter Grave[a]

[a] Archaeomaterials Science Hub, Archaeology & Palaeoanthropology, School of Humanities, Arts & Social Sciences, University of New England, Armidale, NSW, 2351, Australia

[b] Central Science Laboratory, University of Tasmania, Hobart, 7001, Tasmania, Australia

[c] ANSTO, ACNS, New Illawarra Rd, Lucas Heights, NSW2234, Australia

[d] Archaeology Section, Architectural Heritage Dept, Dubai Municipality, PO Box 67, Dubai, United Arab Emirates

ARTICLE INFO

Keywords:
Corroded iron
Recycling
Hot oxidation
Micro-Raman
Southeastern Arabia
Ritual

ABSTRACT

This paper presents an integrated approach to the identification of complex re-processing operations of ancient ferrous artefacts from the multi-period site of Saruq al-Hadid, Dubai, United Arab Emirates. Spatial and morphological studies and a range of archaeometric analyses – optical microscopy, X-Ray diffraction, Micro-Raman spectroscopy, neutron tomography – are used to identify various processing markers preserved in these heavily corroded objects and to distinguish two groups of differently processed fragments. The main analytical focus is the investigation of corrosion layers preserving traces of hot oxidation and forging of metallic iron, along with re-heating of previously formed rust layers. The collected evidence suggests that the numerous iron artefacts ritually deposited at the site in the early Iron Age were subsequently retrieved and re-forged into semi-products as a part of larger scheme of recycling operations, in which Saruq al-Hadid was a first node.

1. Introduction

1.1. The recycling of archaeological metals

Recycling is a defining element of metalworking, but remains one of the least studied and poorly understood aspects of this technology in ancient times. A major reason for the prevalence of this practice is the ability to produce new fully functional objects from deteriorated and non-functional scrap metal (Brown, 1980: 130), and most ancient metal objects must have been 'doomed' to recycling if they were not otherwise removed from circulation, e.g. by deposition in a burial. A wide range of historically-contingent factors could affect the rate and extent of metal recycling, including:

(1) variable demand (e.g. O'Brien, 2016: 61–62), including a strong "seasonal" or episodic demand for metal implements (Moorey, 1971: 84–85);
(2) variable supply, including scarcity of fresh metal due to a lack of local sources (Moorey, 1994: 259–262, Bray et al., 2015: Fig. 4) or disruptions to imports (e.g. Karageorghis and Kassianidou, 1999: 172, Fleming, 2012, Schwab, 2002: 11); and overabundance reflecting the widespread availability of cheap scrap metal (e.g. in colonial Africa, Van Der Merwe and Avery, 1982: 152) or periodic access to large quantities of metal "booty" plundered from graves, battlefields, etc. or received as tribute;
(3) highly corrosive local conditions depleting existing metal stock, such as in African savannas (Gordon and Van Der Merwe, 1984: 109).
These factors could be further compounded by different cultural and aesthetic values and attitudes towards recycling (e.g. Bray and Pollard, 2012: 861).

The ancient use of scrap metal is textually attested across many periods and regions, but is particularly well documented in Mesopotamia. Sources from the third millennium BC refer to copper alloy artefacts from Mesopotamian temples routinely being sent to be remelted and re-fashioned into new artefacts (e.g. Zettler, 1990). Evidence of looting (probably with subsequent re-melting) to obtain booty from military campaigns is similarly commonplace in ancient historical sources, for example in the inscriptions and reliefs of the Neo-Assyrian kings (Millard, 1994: 290–293, Pleiner and Bjorkman, 1974: 291–296).

Unlike the recycling of non-ferrous metals that invariably

* Corresponding author.
E-mail address: ivanstep208@ya.ru (I. Stepanov).

https://doi.org/10.1016/j.jas.2018.11.003
Received 1 June 2018; Received in revised form 23 October 2018; Accepted 15 November 2018
0305-4403/

incorporates re-melting, small-scale recycling of iron involves very different, "solid-state" pathways (Mangin and Fluzin, 2003: 151). These processes are well documented ethnographically (LaViolette, 2000; Pole, 1982; Brown, 1980); LaViolette (2000), for example, writes that in Mali scrap iron was usually sold by weight, although large pieces were more highly valued than smaller pieces because one large piece was often enough to make a fully functional object. Recycled scrap iron was considered of lower quality than objects produced from freshly smelted metal, primarily due to the difficulties associated with forge-welding, decarburization and losses of metal mass. Such processes are also documented in ancient historical sources.

From the Neo-Babylonian period, multiple texts refer to scrap iron, known as *ḫušê AN.BAR*, of various weights, and one such text more specifically refers to "iron for the repair of the plows", suggesting the deliberate combination of old and new metal in an object (Roth, 2005). A Jewish text of the 1st c. AD uses 'scrap' to refer to a broad range of materials, including broken bits of metal utensils which were not easily identifiable, metal scraps split off during manufacturing processes, and broken objects defined by their form and function (Levene and Ponting, 2015).

Although historical and ethnographic evidence indicates that scrap metal recycling was commonplace, such practices are rarely identified archaeologically primarily due to the readily fusible nature of many metals; as noted by Levene and Ponting (2015), "recycling economies, when efficient, are by their nature invisible". Identification of ancient recycling activities thus demands a multifaceted approach that typically integrates different kinds of evidence, including: (a) specific spatio-stratigraphic information, such as the existence of (sorted) piles of metal scrap (Bradley, 1988; Schwab, 2002; Welton, 2016: 229); (b) knowledge of contextual factors such as available resources, exploited mines and networks of supply (Bray and Pollard, 2012; Schwab, 2002); (c) microstructural features of metal artefacts (Schwab, 2002; Welton, 2016: 230–231); (d) specific chemical or isotopic patterns in analysed metal samples (Dungworth, 1997; L'Héritier et al., 2013; Boni et al., 2000); (e) where available, evidence from past written sources (Zettler, 1990; Moorey, 1994).

The present work adopts these criteria to evaluate the evidence for re-processing of ancient ferrous products using a case study from the Iron Age site of Saruq al-Hadid.

Fig. 1. Location of Saruq al-Hadid (up), and its two main sectors of excavations (down): central (C) and northeastern (NE).

1.2. The site of Saruq al-Hadid

Saruq al-Hadid is a multi-period site located in the desert of southern Dubai, U.A.E (Fig. 1). The site is characterised by an unusual material assemblage, including the presence of tonnes of copper slag from primary smelting and secondary refining located away from known sources of ores and possibly fuel (Weeks et al., 2017; Contreras et al., 2017; Herrmann et al., 2012). These metallurgical remains occur alongside numerous high-status and ceremonial objects in copper alloy, iron, gold alloy and other materials thought to have been deliberately deposited as ritual offerings (Contreras et al., 2017; Weeks et al., 2018). The site has produced evidence of ritual activities associated with a snake cult that has widespread parallels in early Iron Age southeastern Arabia (c. 1100-800 BCE; Karacic et al., 2017; Benoist, 2007). Saruq al-Hadid is also one of the only early Iron Age sites in Arabia to contain a significant quantity of ferrous artefact remains – more than 200 kg in total – and this abundance contrasts greatly with the rarity of iron artefacts in the rest of the region (cf. Magee, 1998).

The site's archaeological deposits reflect complex natural and anthropogenic formation processes (Weeks et al., 2017; Herrmann et al., 2012), distributed across different spatio-stratigraphic units. The majority originate from the central sector at the site (Fig. 1, C), where five principal horizons can be distinguished (Weeks et al., 2017). Above the lowest two Bronze Age levels (Horizons IV and V) are three Iron Age and later horizons that produced virtually all of the ferrous materials and metal objects. Horizon I, the uppermost, relatively thin, deflated layer, is largely composed of broken copper slag and associated artefacts and preserves the majority (c. 90%) of ferrous remains (Fig. 2a and b). Horizon II, below, is a thicker layer of loose sand containing a lower proportion of material remains of non-uniform density. Beneath this, Horizon III is an ephemeral but artefact-rich layer that appears to be associated with ritual offering activities (Fig. 2c, Weeks et al., 2018).

A range of absolute dates and typological parallels date Horizons III and II in the central sector of the site to the early Iron Age, c. 1300-800 BC (Weeks et al., 2017: Table 1, Herrmann et al., 2012: 64–65). However, the dating of Horizon I is more difficult due to the complexity of taphonomic conditions at the site, which combine active dunes with heavy deflation of surface deposits. Based on a single OSL date, Herrmann et al. (2012) suggested that metallurgical activities at Saruq al-Hadid post-date the Iron Age (i.e., began after 300 BCE). However, typological analyses of metallurgical residues and radiocarbon and TL dates from Horizons I and II indicate a broad chronological range from the early Iron Age (c. 1000 BCE), through the late Pre-Islamic period (c. 300 BCE – 600 AD), and into the Islamic period (Weeks et al., 2017).

The northeastern sector of the site (Fig. 1, NE) produced another large accumulation of material remains, although the entire deposit of the northeastern sector is thinner (less than 2 m deep) than the deposits of the central sector (up to 6 m). The lower deposits of the northeastern sector are radiometrically and typologically dated to the early Iron Age (Contreras et al., 2017: 62–63), with abundant artefacts that appear to have been associated with ritual activities. The upper deposits of the northeastern sector also contain substantial amounts of primary copper

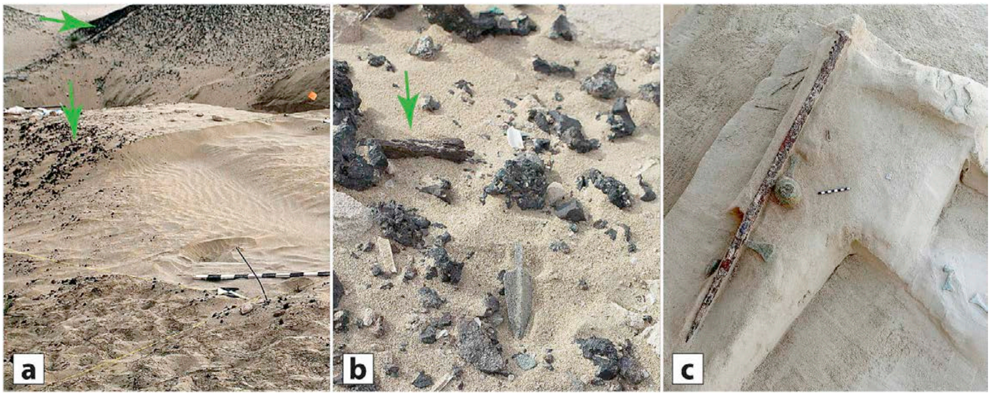

Fig. 2. Horizon I (a, b) and Horizon III (c). **a.** Horizon I. Trench G-T2. Fragmentary deposits of copper slag and ferrous remains (shown by arrows). Excavation by SHARP (Scale bar = 1m). **b.** Horizon I. Close-up view. Ferrous fragment (shown by arrow), copper slag and copper arrowhead. **c.** Horizon III. Trench F-T4. Cluster of ritually deposited copper and iron artefacts. Excavations by Dubai Municipality (Scale bar = 10 cm).

slag and may be of significantly later (younger) age, based on a single C14 date (SRQ14, 1445–1520, 1555–1630 cal. AD 2σ; Contreras et al., 2017: Fig. 4) and limited pottery of Islamic date.

2. Initial indications of iron processing at Saruq al-Hadid

2.1. The typology of ferrous remains

A detailed classification of ferrous remains has been proposed based on the field examination of material from the central and northeastern sectors (Weeks et al., 2017: Fig. 21). The ferrous artefacts from Horizon I are broadly typologically similar to those from Horizons II and III, though Horizon I artefacts tend to be very fragmentary. In total, more than 10,000 ferrous pieces, largely represented by blade fragments, have been excavated form Horizon I. In contrast, Horizons II and III produced around 50 complete swords and daggers (Weeks et al., 2017: Tab. 8).

The fragmentation of iron in Horizon I is ubiquitous, and primarily appears as fracturing of the ends of bladed objects – the average length of a fragment 5–10 cm – while cutting edges and "fullers" are generally intact (Fig. 3). Furthermore, it is usually not possible to find two or more fragments belonging to the same object within a single context of Horizon I, which implies mixing and challenges the alternative interpretation of fragmentation as a product of taphonomic processes.

The majority of iron originates from the central sector of Saruq al-Hadid, whereas the northeastern sector of the site contains only a small iron assemblage of less than 10 kg total weight. Material from the northeastern sector displays a similar range of typologies to that of the central sector but is dominated by small-sized fragments (e.g., of tangs and small blades).

Large and medium-sized ferrous artefacts from Saruq al-Hadid comprise iron swords and daggers that are typologically similar to iron weapons from early Iron Age sites in Luristan, Iran (c. 1100-800 BCE; Overlaet, 2003: Fig. 131). These are characterised by fully metallic flanged hilts and symmetrical mushroom-shaped pommels of variable design (Fig. 4a). The more than 300 fragments of mushroom-shaped pommels and flanged hilts from (secondary) Horizon I contexts indicate the prevalence of ferrous artefacts at the site in the early Iron Age.

In contrast, sword GR7961 (Fig. 4d) recovered from the central sector is characterized by the presence of a mid-rib on both sides of the blade and a partially broken, mushroom-shaped pommel, unlike the rest of the swords from the site which do not have a mid-rib. Typologically similar swords from Luristan are known from the period 800-600 BCE (Haerinck and Overlaet, 2004, Plates 65–69). A further eight fragments excavated from Horizon I contexts in the central sector are characterized by distinct typologies suggesting their production after the early Iron Age. Four of these fragments are pommels of hilts stylized in the shape of an eagle's head (Fig. 4b), with parallels in the late Pre-Islamic period in southeastern Arabia and Iran (Potts, 1998: 197, Yule, 2016: Fig. 32). The other four objects (Fig. 4c) are unparalleled within the ferrous assemblage from the site so far, though one fragment is distinguished by an ornate applique pattern resembling a pattern found on glazed pottery from the late Pre-Islamic site of Ed-Dur in the U.A.E. (Mouton, 2008: Figs. 74, 82). These broad typological parallels are consistent with several late- and post-Iron Age radiocarbon, OSL and TL dates from the site (Weeks et al., 2017, Fig. 6; Herrmann et al., 2012;

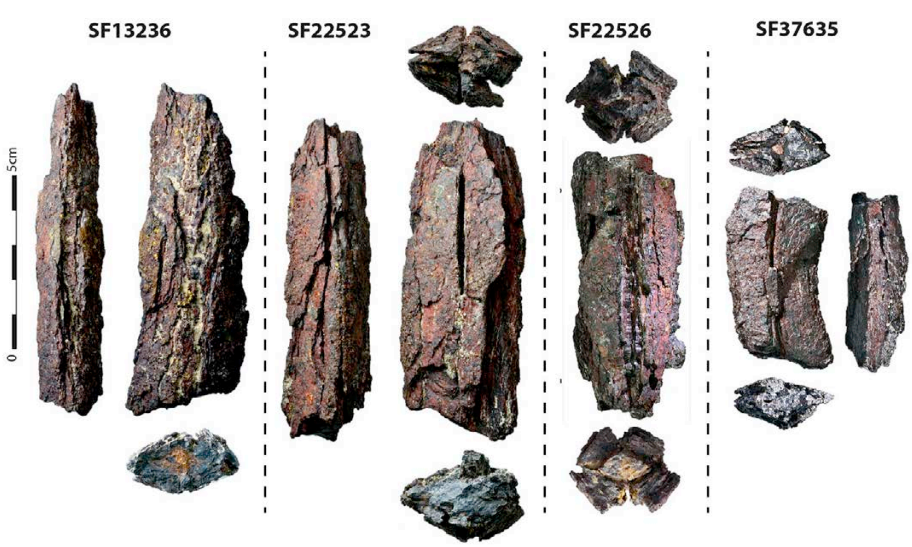

Fig. 3. The typical appearance of fragmented pieces from Horizon I.

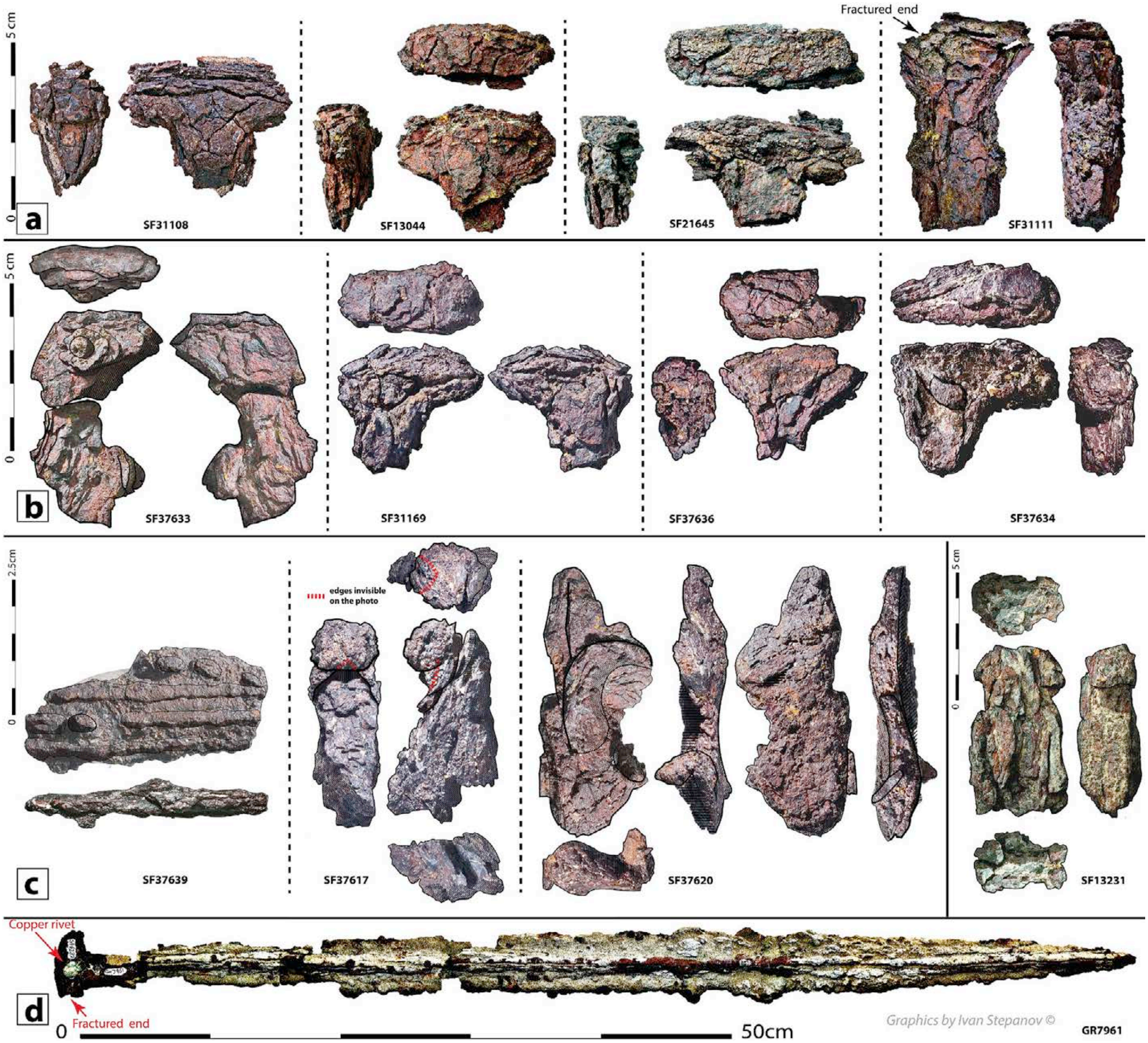

Fig. 4. Typology of Saruq al-Hadid ferrous weapons from Horizon I. **a.** Early Iron Age mushroom-shaped pommels and flanged hilts; **b-d.** Artefacts of "late type": Eagle-shaped hilts (b); various objects (c); mid-ribbed sword GR7961 (d).

Contreras et al., 2017). Overall, it seems appropriate to preliminarily designate these nine pieces from Saruq al-Hadid as "late type" artefacts, implying a broad chronological range extending from the later Iron Age (800-300 BCE) through to the late Pre-Islamic period (300 BCE – 600 CE).

2.2. Spatial markers of processing

Despite the likely late chronology of the "late type" iron fragments, they are found in association with typical early Iron Age objects and with abundant broken copper slag within Horizon I. This ubiquitous co-occurrence of iron and slag in Horizon I of the site, against the significantly smaller amounts of these materials in lower Horizons, highlights the role of the formation processes of Horizon I. Because taphonomic processes such as deflation would be expected to produce substantial heterogeneities in artefact distribution, the exceptionally strong linear correlation observed between iron and copper slag from excavation units in the central sector of the site (Fig. 5) suggests deliberate human agency. This agency could have been retrieval and subsequent processing via disassembly and re-forging of complete objects from Horizons II-III, followed by mixing of a part of the processed residues and their dumping in Horizon I. The typological parallels

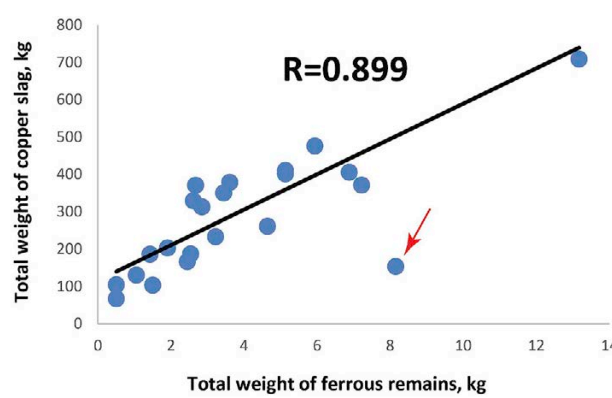

Fig. 5. Spatial marker of processing at Saruq al-Hadid. Linear correlation (R = 0.899) between total weight of copper slag and ferrous remains in the 21 southern SHARP trenches, 5 × 5m^2 from the central sector of the site (mainly Horizon I). The trench outlier (F-S2, shown by arrow) was not included into correlation calculations.

identified between fragments from Horizon I and complete objects from Horizons II-III comprise the first evidence supporting this hypothesis.

2.3. Macro-markers of re-processing

Macroscopic morphological examination is the first stage of a multi-analytical approach to the evaluation of iron processing at Saruq al-Hadid. As iron from Horizon I appears to partly comprise the discarded leftovers of re-processing, visual examination of all fragments permitted a provisional division of the assemblage into two main morphological categories, non-forged and forged.

Non-forged fragments (NFs) represent the majority (c. more than 70%) of examined ferrous remains from Horizon I of the central sector of the site. They display few characteristics of re-processing except for their potentially anthropogenic fragmentation (Fig. 3). Sword GR7964 (Horizon I) displays notches suggestive of exactly such mechanical disassembly as a part of re-processing operations (Fig. 6a).

In contrast, **forged fragments** (FFs) provide morphological evidence of heating, fusion and forging, which are unlikely to reflect the original fabrication of the artefact. Overall, FFs are comparatively less frequent at the site, comprising c. 20–30% of all examined fragments. Heating of these objects can be identified in the extensive exfoliation of their original surfaces, the formation of new bluish oxidized surfaces, and the presence of sandy crusts possibly formed by fusion (Fig. 6d). Similar crusts have been recorded in cremated iron objects from other archaeological sites (Fell, 2004: Fig. 1). Some bladed objects look compacted (Fig. 6b), while the others are characterized by widely-spread channels in place of fullers and cutting edges (Fig. 6c), a previously unattested manufacturing technique likely caused by secondary processing/disassembling operations.

Blade fragments, representing the majority of the ferrous remains, can be grouped by the dimensions of their cross-section into large (cross-section > > 20 mm x 16–20 mm), medium (cross-section 15-20 mm x 13–16 mm) and small (cross-section < < 15 mm x 12–14 mm) pieces. Most of the large FFs originate from the central sector of the site and typically comprise massive double- and single-edged fragments or larger knives, daggers and swords, often heavily deformed. Medium and small FFs were recovered from both the central and northeastern sectors, dominating the iron assemblage in the latter location, and are consistent with the processing of original objects such as smaller tanged

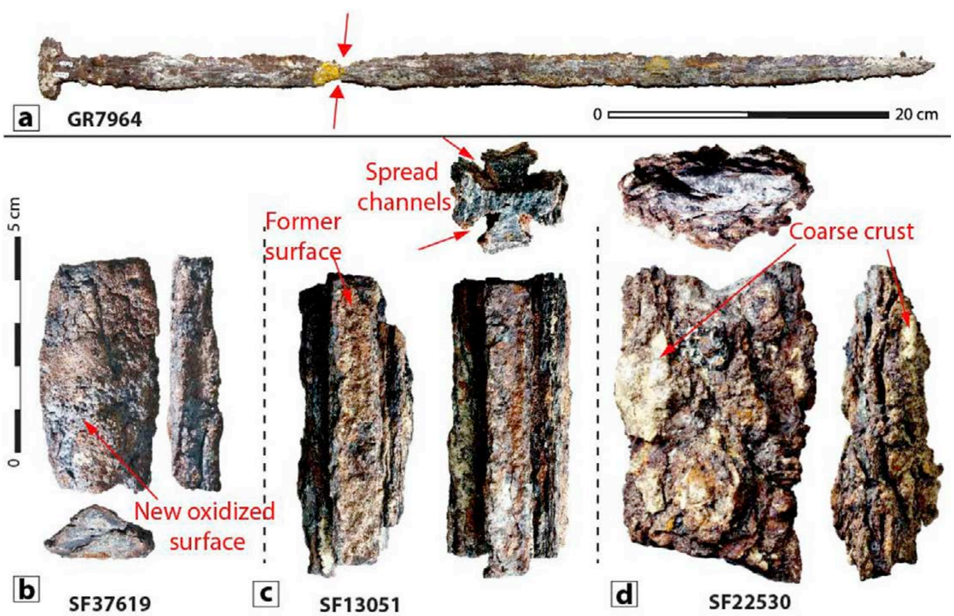

Fig. 6. Typical morphologies of processed fragments and markers (shown by red arrows). **a.** Partially disassembled sword as evidenced from the presence of notches (shown by red arrows). GR7964. **b.** Compacted fragment. SF37619. **c.** Channelled fragment. SF13051. **d.** Fragment with coarse crust. SF22530. (For interpretation of the references to colour in this figure legend, the reader is referred to the Web version of this article.)

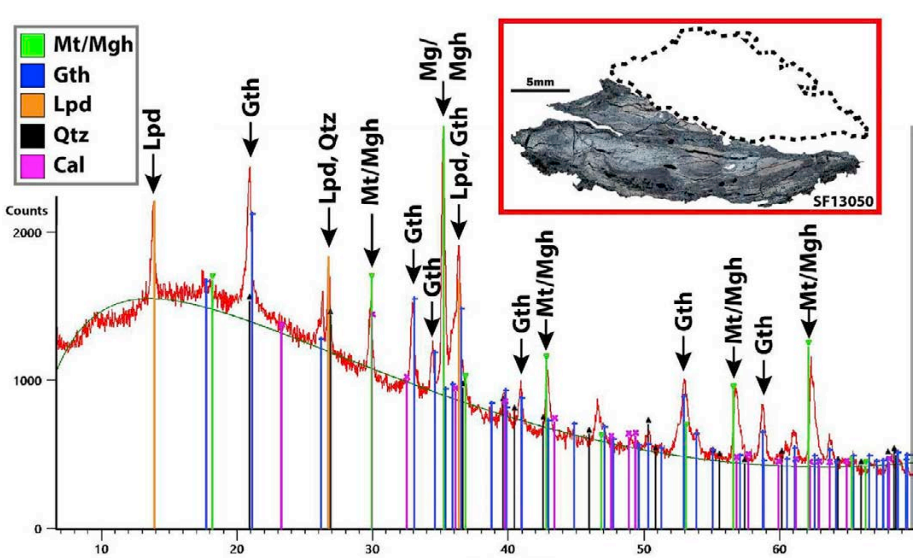

Fig. 7. XRD spectrum of a typical forged fragment SF13050, obtained from the half of the cross-section shown in the red rectangle (OM BF image). The spectrum reveals the presence of magnetite/maghemite phase (Mt/Mgh), goethite (Gth.), lepidocrocite (Lpd.), and small amounts of quartz (Qtz., probably from the surface crust) and calcite (Cal., probably pore infill). (For interpretation of the references to colour in this figure legend, the reader is referred to the Web version of this article.)

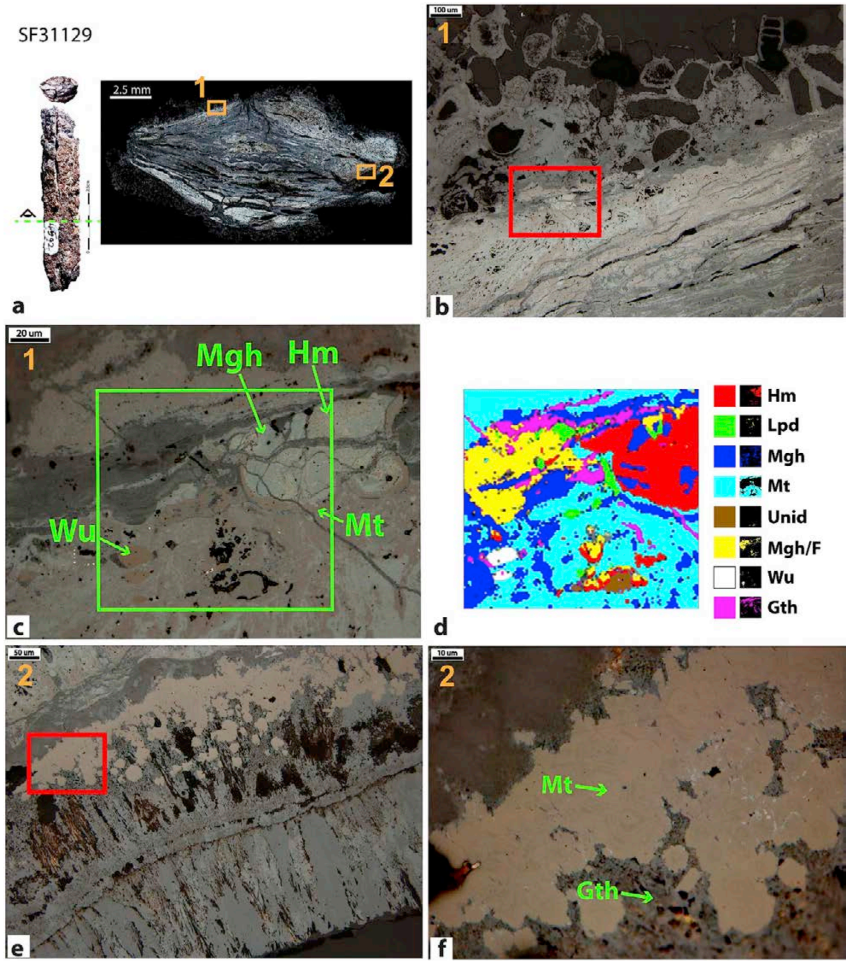

Fig. 8. SF31129. Outer corrosion layers in areas #1 and #2. **a.** photo and overview OM BF image; **b.** Area #1; **c.** Hot oxidation feature shown in the red rectangle in *b*; **d**. Micro-Raman map with identification of corrosion phases: hematite (Hm), lepidocrocite (Lpd), maghemite (Mgh), magnetite (Mt), unidentified phase (Unid), poorly crystalline maghemite/ferrioxide (Mgh/F), wustite (Wu), goethite (Gth); **e.** Area #2; **f.** Magnified area from *e.* (For interpretation of the references to colour in this figure legend, the reader is referred to the Web version of this article.)

knives and spearheads.

These macro-markers suggest that re-processing operations at Saruq al-Hadid could have consisted of the disassembly of complete objects through heating and mechanical working. This general hypothesis is explored using a range of materials analyses in the following sections.

3. Materials and methods

All ferrous artefacts from Saruq al-Hadid are heavily corroded due to the highly aggressive local burial environment, although some display preserved 'islands' of metallic iron (< 300 μm) visible after sampling. Despite the serious analytical difficulties introduced by such poor preservation, recent research demonstrates that an appropriate suite of archaeometric methods can provide insight into the initial manufacturing techniques and provenance of these objects (Stepanov et al., 2018a; Stepanov et al., 2018b). Specifically, optical microscopy enables investigation of remnant carburized structures within different parts of the sample, SEM enables compositional analysis of unaltered slag inclusions from the smelting process and neutron tomography enables investigation of forge-welding techniques. The present work, in contrast, focuses upon analytical approaches to better understand the evidence for re-processing of heavily corroded iron artefacts.

Detailed evaluation of forging during re-processing derives from the microstructural analysis of 90 iron fragments from the site: 82 from Horizon I in the central sector and 8 from upper deposits of the northeastern sector of the site (photos and microstructures are reported in Supplementary #1). High-resolution investigation of morphology and micro-structure, especially corrosion layers, was used to confirm the re-processing steps suggested by macroscopic visual examination.

3.1. Investigation of microstructure

Optical microscopy (OM), X-ray diffraction (XRD) and Micro-Raman analyses were used to evaluate the prominent outer exfoliated and oxidized layers first identified macroscopically, allowing corrosion products most likely formed rapidly during high-temperature heating to be differentiated from corrosion products associated with long-term environmental degradation (Neff et al., 2005). Specifically, these studies identified a rapidly formed layer (so-called "calamine"), consisting of several different oxides, including magnetite, hematite and wustite, sometimes reported for artefacts subjected to hot forging or cremation (Bouchar et al., 2013: 369, Dungworth and Wilkes, 2007; Golfomitsou et al., 2017), and typically located at the limit of the artefact's original surface (i.e., the outer surface that existed prior to long-term corrosion). As a means to differentiate ferrous fragments based on their different corrosion patterns, the amount of the total surface area (%) of white and light-brown to pink reflective corrosion phases (consisting of magnetite, maghemite and in some cases hematite, see sections 4.1, 4.2) was calculated for each sample.

SEM analyses were conducted to determine if the surface crusts present in FFs were formed as a result of high-temperature fusion or long-term burial. This was particularly important, as ferrous artefacts

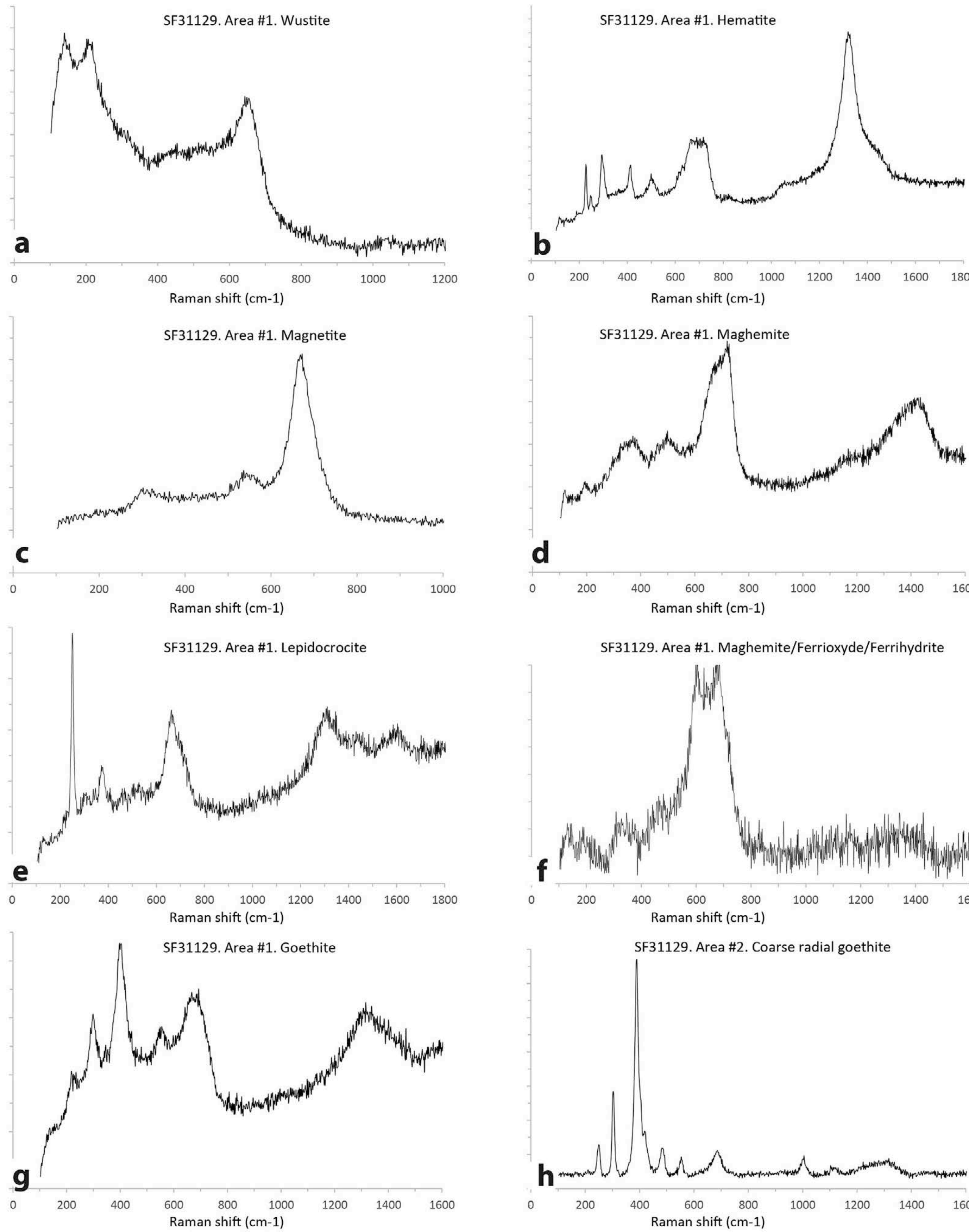

Fig. 9. Raman spectra of corrosion phases from SF31129. **Area 1 (a–g): a.** Wustite; **b.** Hematite; **c.** Magnetite; **d.** maghemite; **e.** Lepidocrocite; **f.** Poorly crystalline maghemite/ferrioxide/ferrihydrite; **g.** Goethite; **Area 2: h.** Coarse radial goethite.

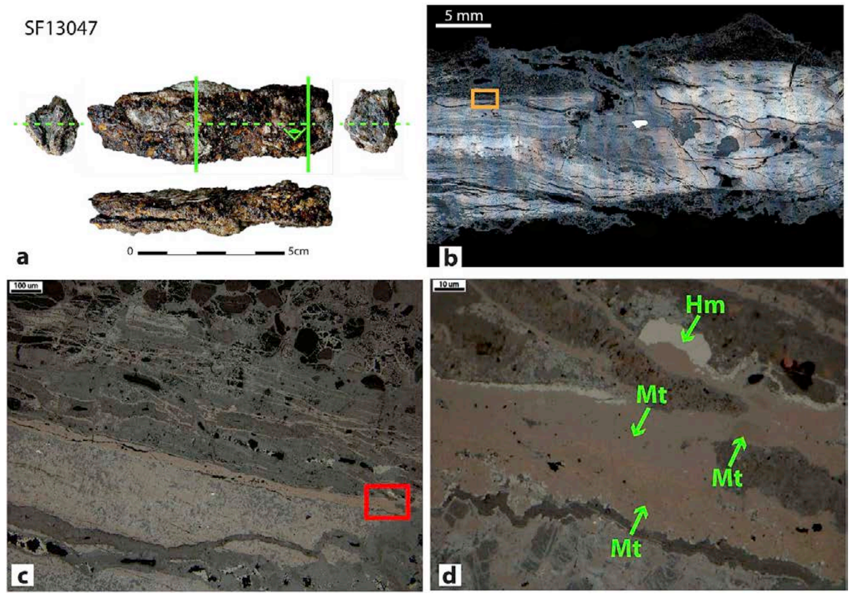

Fig. 10. SF13047. Outer corrosion layers. **a.** photo; **b.** Overview OM BF image; **c.** Hot oxidation layer; **d.** Magnified area of the red rectangle from *c* with designated phases. (For interpretation of the references to colour in this figure legend, the reader is referred to the Web version of this article.)

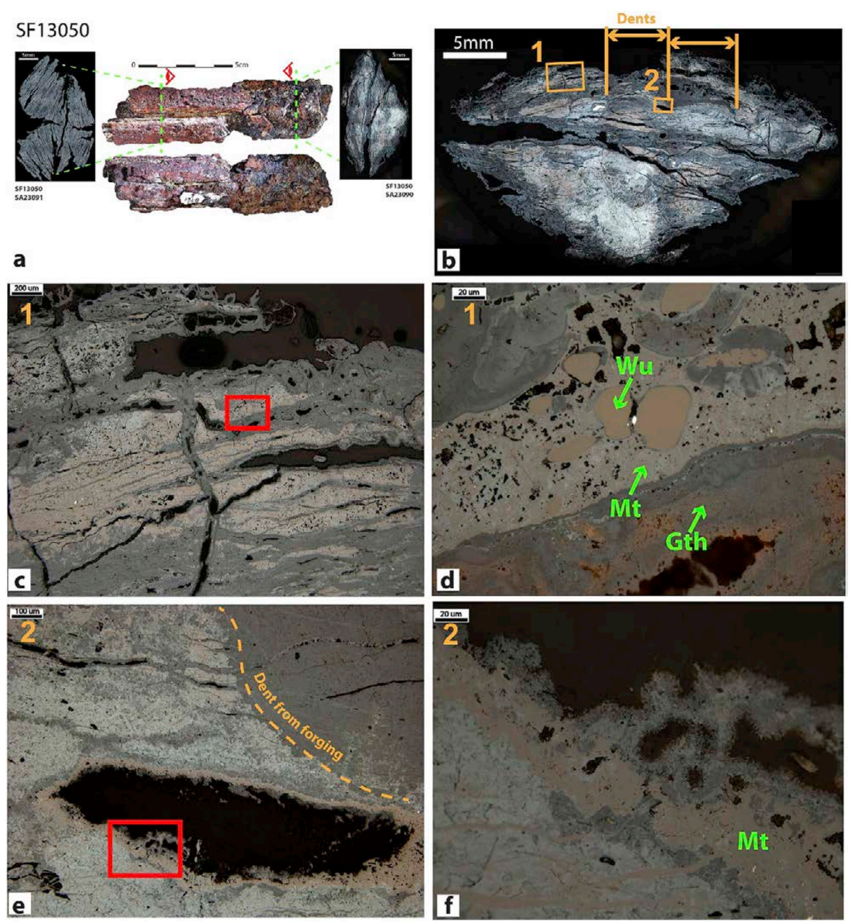

Fig. 11. SF13050. **a.** Photo and overview OM BF images; **b.** Overview OM BF image of a forged end. Areas #1 and #2 are indicated by rectangles. Dents embedded into magnetite/maghemite layers are indicated by arrows. **c.** Area #1; **d.** Magnified area from *c*; **e.** Area #2; **f.** Magnified area from *e*.

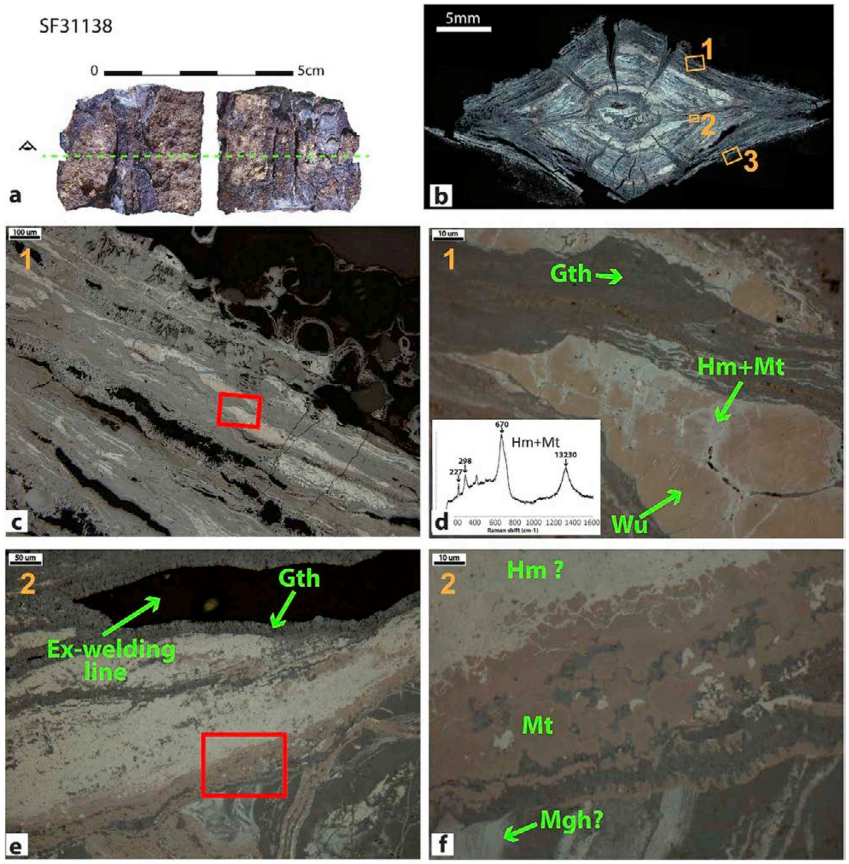

Fig. 12. SF31138. **a.** Photo; **b.** Overview OM BF image. Areas #1, #2 and #3 are designated by rectangles. **c.** Area #1; **d.** Magnified area from *c*; **e.** Area #2; **f.** Magnified area from *e*.

that have undergone long-term corrosion in soil are known to have an outer layer (the so-called "Transformed Medium") naturally incorporating mineral grains from the burial environment (Neff et al., 2005). Finally, the presence of other specific features possibly associated with recycling, such as spheroidized cementite particles (Kusimba et al., 1994: 73), was also assessed.

3.2. *Investigation of plastic deformation "dents"*

Given the macroscopic morphological evidence of shape deformation in FFs, more detailed examination by neutron computed tomography and OM was conducted to identify surface and matrix characteristics of the plastic deformation. Neutron tomography, owing to its non-invasive nature and capability for an accurate 3D mapping of bulk morphological and structural features, was used for the identification and investigation of "dents" within an initial set of 14 objects, while OM was used to invasively investigate the remaining 76 objects. For details of neutron tomography operational settings, see Supplementary #2. Only objects with at least 6–8 identifiable dents were included into the final results. Ultimately, the purpose of this investigation was to distinguish between hammering from the original manufacturing processes and hammering from the secondary re-processing operations for FFs (n = 9) and NFs (n = 16).

4. Results. Micro-markers of processing

Microstructural markers of processing were ubiquitous in macroscopically identified FFs, confirming that their mechanical working history and mechanisms of degradation were different from the fragments identified as NFs. As discussed below, the re-processing markers identified in FFs include corrosion products associated with hot oxidation and re-heating of rusty fragments, surface crusts formed by hot adhesion of sand, and dents from mechanical re-working.

4.1. *Products of hot oxidation*

4.1.1. *XRD analysis*

OM examination indicates that the structure of NFs is dominated by a low-reflective, grey corrosion product of iron oxi-hydroxide, while FFs contain in addition varying amounts (usually 20–50% of surface area) of reflective white or bluish-white and light-brown corrosion phases. These phases were initially identified as magnetite and/or maghemite, based on the nature of iron corrosion in sediments (Neff et al., 2005) and the alkaline burial environment at Saruq al-Hadid (i.e., pH of ~8.0–9.0, cf. Uqba, 1991: Tab. 2.6). An X-ray powder diffraction pattern for part of a forged fragment SF13050, confirms the OM identification of a magnetite/maghemite phase (the precise discrimination between two phases not possible with the chosen XRD method), and iron oxi-hydroxide phases of goethite and lepidocrocite (Fig. 7, details of XRD setup are reported in Supplementary #2).

Overall, none of the phases identified by XRD can exclusively attest to the hot oxidation of iron relevant to the scope of the present study. While magnetite can form as a product of high temperature oxidation (Kubaschewski, 2013), this phase is also a common product of the long-term corrosion of iron in soil (Neff et al., 2007).

In contrast, successive layering of metastable wustite, magnetite and metastable hematite near the surface of the object can be considered as a reliable indicator of the hot oxidation processes (Buchar et al., 2013: 364, Dungworth and Wilkes, 2007). These outer 'hot oxidation layers' containing phases of magnetite, hematite ± wustite were preliminarily identified in 12 out of 28 FFs under OM, and were confirmed in four samples (SF31129, SF31138, SF13050, SF13047) by Micro-Raman

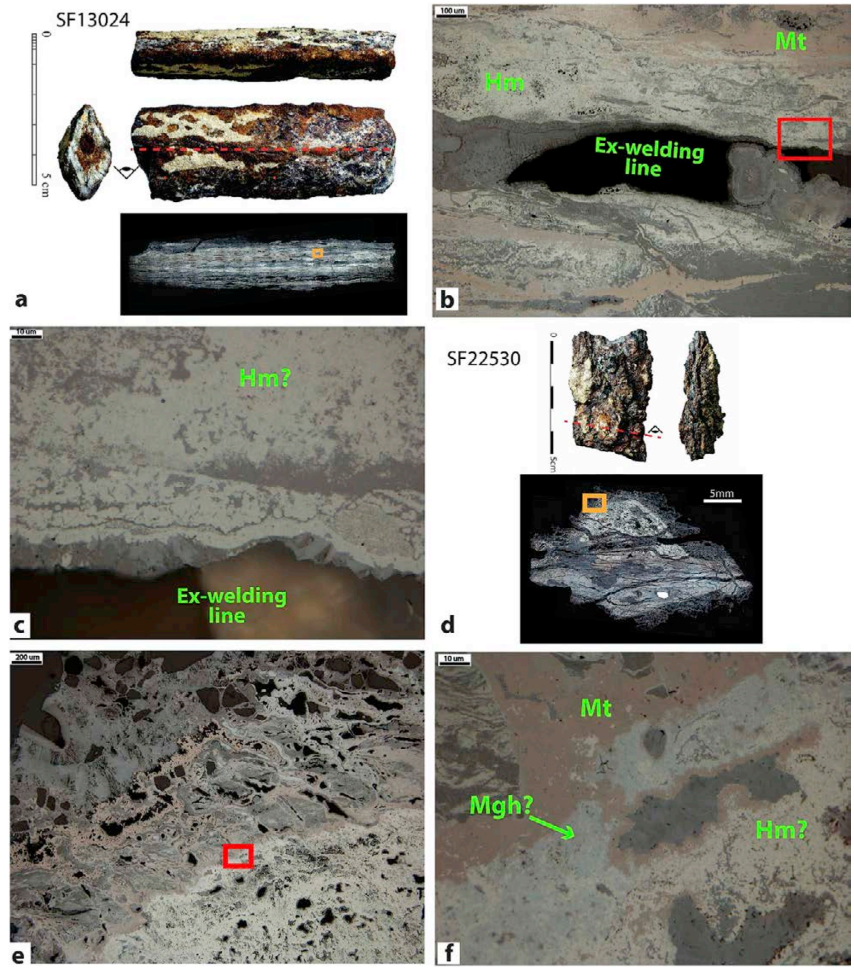

Fig. 13. Possible presence of hematite in the objects. **a.** SF13024. Photo and OM BF overview image; **b.** Area of the orange rectangle from *a*; **c.** Magnified area from *c*; **d.** SF22530. Photo and OM BF overview image; **e.** Area of the orange rectangle from *d;* The orientation of pores indicates forging. **f.** Magnified area from *e.* (For interpretation of the references to colour in this figure legend, the reader is referred to the Web version of this article.)

analyses (details of chosen Raman setup are reported in Supplementary #2).

4.1.2. Micro-Raman analysis

In area #1 of the sample SF31129, (Fig. 8a), the hot oxidation features occur near the transformed medium composed of soil grains cemented with iron oxi-hydroxide (Fig. 8b). The feature itself contains hematite ex-solved with maghemite outlined by a high-relief magnetite layer (3–5 μm thick, Fig. 8c). Globular wustite is present near that feature and could have also formed from hot oxidation or from forging (as a component of a slag inclusion). The Raman map (Fig. 8d) reveals that the main phases of the corrosion matrix, which embed the hot oxidation features, appear to be magnetite, maghemite, goethite and a component near the exterior surface of the object, which may be a poorly crystalline species of maghemite, ferrioxide or ferrihydrite, based on the presence of two shoulders on the broad band at 600 and 680 cm^{-1} (Fig. 9f, Neff et al., 2006).

A different area (#2, Fig. 8e) within the same sample SF31129 features a layer of euhedral magnetite, as identified by Raman, with pronounced zoning (Fig. 8f), followed by a coarse radial goethite grown perpendicularly to the surface. Narrow Raman bands of radial goethite (Fig. 9h) indicate that it is a well-crystalline phase. Overall, such morphology and good crystallinity of magnetite and goethite is a result of a change in the physico-chemical environment of mineralization over time that indicates a slow (during burial), rather than fast (upon heating), crystallization process. However, considering the above-discussed evidence for surface hot oxidation of the sample in area #1, the preferentially oriented nuclei of magnetite could have already formed at a microscopic level upon the hot oxidation of metallic iron at temperatures > 500 °C as would be the case for the other oxides (Marciuš et al., 2012). It can be further suggested that these preferentially orientated magnetite nuclei promoted the growth of new magnetite zones and subsequent radial goethite during the subsequent burial period.

The sample SF13047 (Fig. 10c) has a more uniform and continuous hot oxidation layer (30–50 μm thick) developed close to the transformed medium, and consisting of magnetite and an outer rim of hematite (Fig. 10d). The different colour tones within the magnetite layer have identical Raman spectra implying similar crystal structure, but a different crystal orientation of magnetite, which is probably due to the rapid rate of the hot oxidation process.

The sample SF13050 (Fig. 11a) is a peculiar example of an object that was forged on one side but not on the other, as seen from the different microstructures of its ends. In the forged part of the object (Fig. 11b), the old exfoliated layer is almost totally absent, with only newly oxidized surface exposed. The object's forged end whose half was investigated by XRD as bulk (section 4.1.1), contains lenticular features, 5–7 mm long, near the new surface (Fig. 11c), and inside the object that are interpreted as dents from hammering. One, as identified by Raman, is composed of wustite in a matrix of magnetite (Fig. 11d), and was probably formed due to hot forging and hot oxidation. Similar lenticular features occurring inside the object do not contain wustite

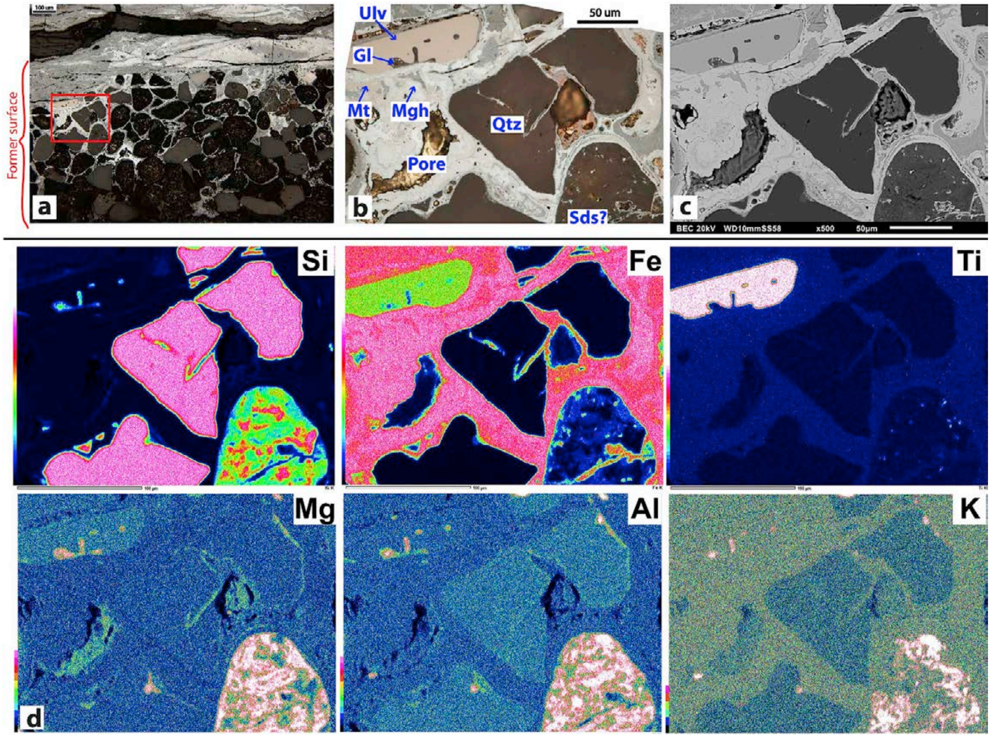

Fig. 14. Fused sandy layer of SF31138. Area #3 from Fig. 13b. **a.** Overview OM BF image from a sandy layer; **b.** Magnified area from *a*. OM BF image with designation of components: magnetite (Mt), maghemite (Mgh), ulvöspinel (Ulv), glass (Gl), qartz (Qtz), pores from former Ca-Mg carbonate and possible sandstone (Sds); **c.** SEM BE image; **d.** SEM-map. Distribution of element contents within the chosen area.

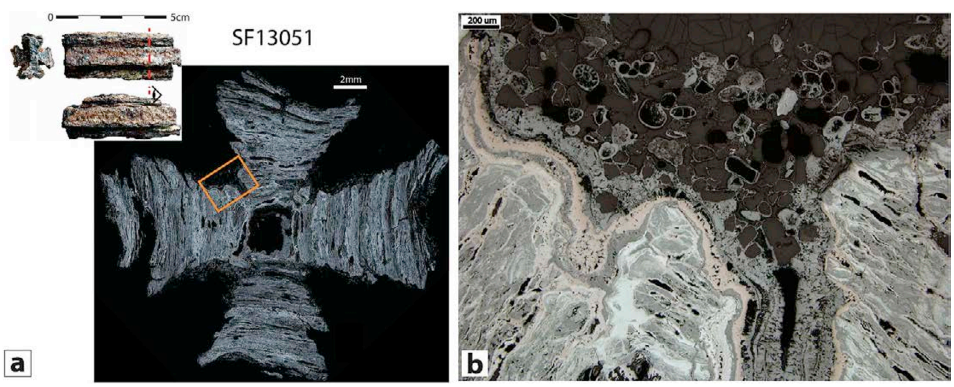

Fig. 15. Channelled object SF13051. **a.** OM BF overview image; **b.** Magnified area from *a*.

(Fig. 11e and f), indicating that they were largely un-affected by hot oxidation except for the possible formation of microscopic magnetite nuclei inside adjacent cracks and weakly consolidated welding lines, which were infiltrated by oxygen during hot forging. As in the case of sample SF31129, these magnetite nuclei in areas that absorbed the majority of thermomechanical impact from hammering could have promoted further growth of magnetite and maghemite during the subsequent burial period. This theory therefore can explain the differences in the corrosion patterns observed in forged and non-forged parts of the object SF13050.

Finally, the sample SF31138 (Fig. 12a and b) is a fragment of two-edged sword with an internal layered distribution of iron oxides preferentially oriented to the features that are possible former welding lines. In area #1, near the outer surface of the object, a feature (30–60 µm thick) consisting of wustite with ex-solved white lamellae was identified (Fig. 12c and d). The Raman spectrum of the white lamellae reveals the main band of magnetite (660 cm^{-1}) and minor bands of hematite (1330, 227, 298 cm^{-1}), which can possibly indicate microscopic mix of these two phases and is consistent with their successive formation during the hot oxidation of iron.

Overall, the character of hot iron oxidation layers present near the surface of FFs is peculiar. While the process of hot iron oxidation cannot be denied, the layers formed in most samples are localized, discontinuous and often quite thin. This may reflect the fact that the objects were often re-processed at relatively low temperatures (i.e., below 900 °C), or the possible removal of the hot oxidation layers by subsequent hammering.

4.2. Evidence of re-heating of initial rust/corrosion layers

The investigation of internal cracks outlining the former welding lines of object SF31138 (area #2, Fig. 12e) reveals three successive layers: colloform goethite growing form the walls of the crack, followed by a thick white layer (100–250 µm), which is probably hematite based on similar optical properties for hematite identified by Raman spectroscopy in area #1, followed by a layer of euhedral magnetite (30–40 µm, Fig. 12f). In the other object (SF22530, Fig. 13d), the large areas of hematite are located close to the surface, although are not associated with wustite (Fig. 13e and f). These patterns are generally not expected during burial corrosion, nor do they seem to have formed by the hot oxidation of metallic iron. Instead, if the iron object was already partially rusted and the main component of rust (Fe[III]

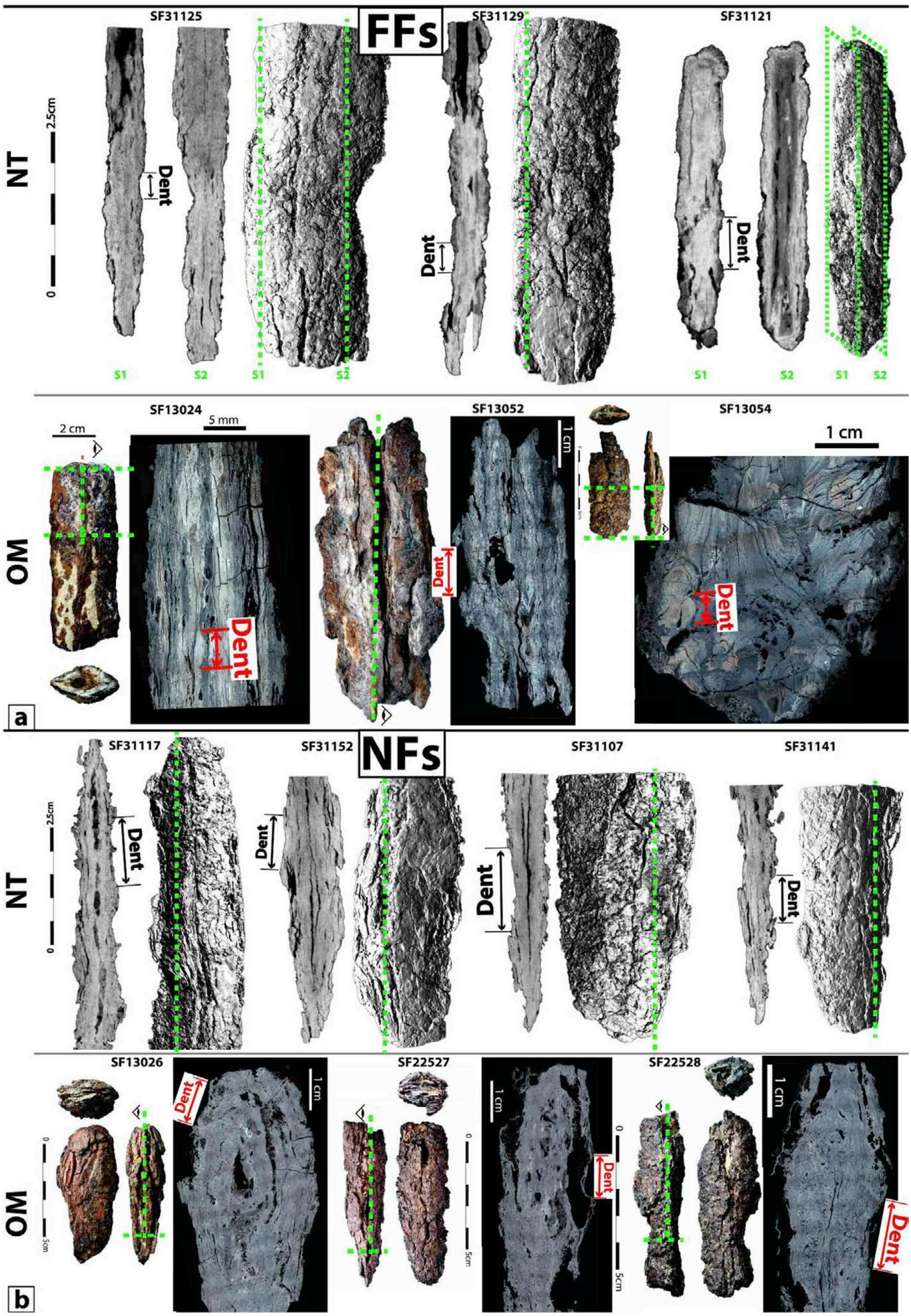

Fig. 16. Typical appearance of dents in NFs (a), and FFs (b) from Saruq al-Hadid based on examination by neutron tomography (NT) and optical microscopy (OM).

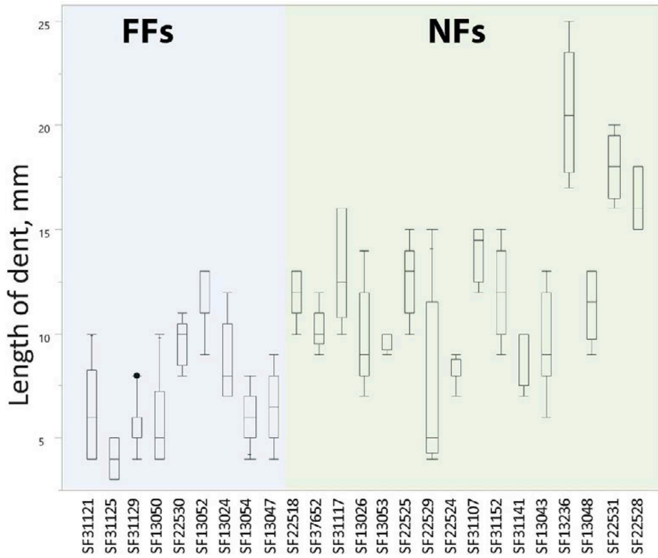

Fig. 17. Box plot of variation of the length of dents in NFs, and FFs.

goethite) had formed on the surface and within the cracks, re-heating of the object, accompanied with infiltration of oxygen into cracks, would convert existing goethite to hematite, which would explain the unusual corrosion pattern, which is attested for a large number of FFs (13). As to the cause for the initial vulnerability of the ex-welding lines in FFs (i.e., during initial manufacturing of the objects), it may relate to the combined effect of imperfect early Iron Age forge-welding, with lack of temperature control (Stepanov et al., 2018b), and subsequent preferential degradation of these unstable areas during use and initial burial of the objects.

4.3. Fused surface crusts

The investigation of the sandy crusts formed on the surface of FFs reveals considerable variation in their thickness (from 0.2 to 5.0 mm), both within a single artefact and between different artefacts. These sandy crusts usually occur at the former outer surfaces of the objects due to hot adhesion or fusion, as seen from the alteration of sand grains and their association with magnetite and maghemite, as identified by Raman, in one sample (Fig. 14a and b). The alteration of sand grains is attested through cracking and partial melting. The melting is pronounced for most of the observed minerals (i.e., calcite, feldspar, Mg-Fe pyroxenes, ilmenite, Howari et al., 2007) except for quartz, which is only lightly melted at the exterior (Fig. 14d). In individual cases, the melting of sand is indicated by the crystallization of ulvöspinel (identified by Raman spectroscopy and elemental analysis) and the formation of residual glass, which implies temperatures in the range 1000–1200 °C. In the channelled object SF13051 (Fig. 15a), the thickest layer of sand (~1 mm) is accumulated inside the channels and embedded into magnetite and goethite layers (Fig. 15b).

4.4. Dents from mechanical working

Application of OM and neutron tomography revealed the presence of different types of dents on the surface of different categories of iron artefacts (full details are reported in Supplementaray #3). The dents detected in 9 FFs are generally smaller (avg. = 7 mm, Figs. 16a, 17), while the dents on 16 NFs are generally larger (avg. = 12 mm, Figs. 16b, 17). This indicates that, in the case of FFs, tools with a small working face, such as punches or small hammers, were preferred over larger tools. Furthermore, the dents found in NFs are usually not embedded into magnetite and maghemite layers as is the case of most of FFs (Fig. 11e), but instead preserved only as surface indentations. These data once again emphasise differences in the working histories of FFs and NFs, suggesting that small dents distributed across FFs resulted from re-processing, while the larger dents found on the surface of NFs probably reflect their original fabrication.

4.5. Other features

Additionally, 11 out of 62 NFs also contain structures of small (ca. 1 μm) spheroidized cementite (Fig. 18), precipitated around ferrite grains of fairly large size 50–200 μm. Although the metal is fully corroded, the selective mechanism of corrosion (i.e., in preference to ferrite) suggests that preserved pseudomorphs correspond to a single ferrite grain and not to an agglomeration of grains. Overall, the revealed features usually occur near the outer surfaces and less commonly in the object's core. The association between the mentioned type of grains near the surface and spheroidized structures indicates that considerable cold deformation preceded the prolonged heating of the objects (Gordon and Van Der Merwe, 1984: 112). While spheroidized structures are sometimes reported for objects suspected to have been fabricated from old rusty scrap via several hours of re-forging (Pole, 1982: 507, Kusimba et al., 1994: 73), these structures are also common in non-recycled objects forged below 727 °C (Samuels, 1980). Furthermore, the structures of spheroidized cementite and large grains (although not always in direct association with each other) are reported for decorated swords from the Luristan region (Smith, 1971), the possible provenance of the Saruq al-Hadid objects based on typological and compositional parallels (Stepanov et al., 2018b; Stepanov et al., in prep.). This observation, along with the almost total absence of spheroidized structures in FFs, indicates that the observed spheroidized structures are unlikely to have been caused by re-processing operations.

4.6. Summary

Macro- and micro-markers, summarized in Table 1 (full details are reported in Supplementary #4), indicate consistent differences in the corrosion patterns and processing histories of NFs and most of FFs. In

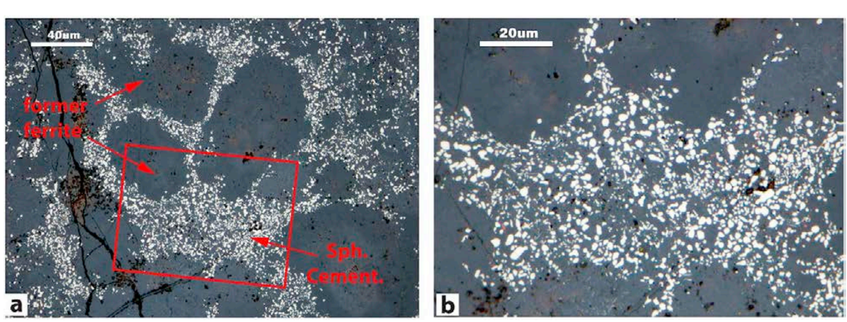

Fig. 18. OM BF. Structures of spheroidized cementite precipitated around former ferrite grains. SF22525. **a.** Area near the surface of the object; **b.** Magnified area from *a*.

Table 1
Macro- and micro-markers of processing in different types of fragments based on the investigation of 90 artefact samples from Saruq al-Hadid.

N artefact samples	Type of processing	Sector of the site		Macro-markers of processing				Micro-markers of processing					
				Fractured ends	Distorted shape	Exfoliation of former surfaces	Fused sandy crusts	Mt, Mgh and Hm, % area in sample		Successive layers Mt, Hm ± Wu on the surface	Thick layers of Hm at the surface/along ex-welding lines	Dents on the surface/in the structure	
		Central	NE					$\bar{x}$	σ			$\bar{x}$, mm	σ
62	NF	62	0	58	2/62	2/62	1/62	8 (outlier = 70)	6 (n = 44)	0/45	0/45	12 (n = 16)	1.8
28	FF	20	8	24	11/28	24/28	20/28	37	17	12/28	13/28	7 (n = 9)	1.5

NF: non-forged fragment; FF: forged fragment; Mt: magnetite; Mgh: maghemite; Hm: hematite; Wu: wustite

contrast to NFs, FFs typically contain significantly larger amounts of magnetite and maghemite and often preserve evidence of hot forging and hot iron oxidation at their surface, accompanied by fused sandy crusts. Significant numbers of FFs incorporate thick layers of a white corrosion phase, likely hematite formed by the reheating of the initial rust from the surface and cracks of the partly degraded objects, which would have happened if the ferrous objects originally ritually deposited in Horizons III and II were retrieved and re-worked. Finally, the dents identified in FFs are often embedded into their corrosion products of magnetite and maghemite and represent processing with smaller tools, as opposed to NFs, which do not embed any dents into their corrosion layers, but contain only surface indentations of a larger size indicating that their original manufacture utilised larger tools. Overall, as seen from the finds such as SF13050 (Fig. 11a) – which consisted of one forged and one non-forged end characterized by different corrosion patterns – and from the results of archaeometric analyses, the corrosion patterns of NFs seem to be influenced only by burial conditions, while the corrosion patterns of FFs are influenced both by burial conditions and by subsequent thermomechanical processing.

5. Discussion

The ferrous assemblage of Saruq al-Hadid represents a unique, significant, but complex and enigmatic aspect of the history of early Iron Age south-eastern Arabia. The ferrous fragments from the mixed and deflated deposits of Horizon I at the site present the greatest challenge to interpretation, in particular understanding the technological processes that contributed to the formation of those remains identified as forged fragments (FFs). Superficially, these objects appear to be unfinished or semi-processed products, which bear traces of rough working with thick masses of sand fused to their surface, which is perhaps not unexpected for the outputs of a desert production site. However, the results of archaeometric analyses from the present study combined with the socio-technological context of Saruq al-Hadid and South-eastern Arabia challenge this hypothesis.

Overall, there are two possible explanations for the formation of FFs and their presence at Saruq al-Hadid. As discussed below, the authors favour the interpretation that FFs represent the re-processing of complete objects previously ritually deposited at the site. However, the alternative possibility – that FFs are the by-product of iron manufacturing operations carried at Saruq al-Hadid – requires discussion. This theory is challenged on several fronts, however, both technical and archaeological. Most significantly, there is a total absence of iron smithing slags or hammer scales at Saruq al-Hadid, despite more than 10 years of excavation at the site that have recovered more than 200 kg of ferrous remains. In contrast, several smithing slags have been observed from the broadly contemporary early Iron Age settlement site of Muweilah in the U.A.E. (Stepanov et al., in prep.), a good indicator that small-scale secondary metalworking was undertaken there. Moreover, the fabrication at Saruq al-Hadid of 1 m long iron swords, discovered in the lower Horizons of the site, is particularly unlikely. Producing these artefacts would have required advanced forging skills which, in the early first millennium BCE Near East, probably only existed in the royal smithies of Assyria (Pleiner, 1979) and the metalworking centres of western Iran (Thornton and Pigott, 2011; Rehder, 1991: 15), based on the significant number of iron finds from these regions and results of metallographic examinations.

Consideration of the broader socio-technological context of early Iron Age South-eastern Arabia also raises serious doubts regarding the likelihood of local iron production. Significantly, field research in this region since the late 1970s has identified a significant dearth of iron objects at almost all early Iron Age sites – with the exception of Saruq al-Hadid. Such doubts are further reinforced by the fact that the iron (and some copper alloy) swords and daggers discovered at Saruq al-Hadid and other sites in the region (Gernez , 2018: 96, Fig. 7.13, Lombard and Kervran, 1989: Fig. 145) display distinct typological

Table 2
Macro and micro-markers, type and possible cause for re-processing of complete objects at Saruq al-Hadid.

Category	FFs: forged fragments	NFs: non-forged fragments
Macro and micro-markers	Compacted with traces of rough forging or channelled shape; Exfoliation of former surfaces; Masses of sand fused to the surface; Magnetite/maghemite, often distributed along the ex-welding lines; Hot oxidation products and thick layers of hematite; Dents from smaller tools embedded into magnetite	Fractured ends, while the cutting edges and fullers are generally intact; Dents from larger tools on the surface; Absence of fused sandy crusts and hot oxidation layers; Localized structures of spheroidized cementite
Type of processing after breaking	Heating and forging using small tools, possible work aimed at the removal of the already formed rust	Discard
Possible cause of processing (FFs) or discard (NFs)	Best state of preservation or largest amount of preserved metal.	Low amount of preserved metal

parallels to objects from Luristan (Overlaet, 2003: 156, Fig. 123, Muscarella, 1988: Fig. 219). Along with the investigation of remnant carburized structures (Stepanov et al., 2018b) and ongoing geochemical analyses (Stepanov et al., in prep.), the evidence suggests that the Saruq al-Hadid artefacts were imported to South-eastern Arabia as finished objects, probably after their manufacture in Western Iran. The fabrication at the site of smaller objects not requiring advanced forging skills is possible, although the absence of smithing slags is still to be addressed in such a scenario.

As noted above, the second theory regarding the interpretation of FFs is that they represent the re-processing of complete objects initially ritually deposited in Horizons II-III of the site and retrieved sometime after their initial deposition for the purpose of re-forging and recycling. This hypothesis, although preferred by the authors over the "manufacturing theory", can also be contested. The first aspect is character of the re-processing thought to have been undertaken, which is not recycling as commonly understood in archaeometallurgical studies (Bray et al., 2015; Schwab, 2002) characterized by the manufacture of finished objects from the forge-welding of different scrap fragments, resulting in a mixed compositional signature. Instead, the characteristics of the FFs from Saruq al-Hadid suggest the early, probably preliminary, stages of recycling involving retrieval, assessment and initial reworking operations. The performance of subsequent welding of smaller pieces into larger ones – the expected later stages of recycling – is not directly supported by any evidence found on site.

The rationale for the processing of objects identified as FFs, and the non-processing of objects identified as NFs other than their possible fragmentation, is also difficult to reconstruct. The sorting of iron fragments by size and possibly by degree of preservation could have been an important component of recycling operations at Saruq al-Hadid, with parallels in the ethnographic literature (e.g., LaViolette, 2000; Pole, 1982). The domination of mostly small and medium-sized FFs in the iron assemblage of the northeastern sector also strongly suggests deliberate sorting. This fragmentation (breaking) attested in NFs in turn could have been a deliberate act to evaluate the amount of metal preserved in the core of the object and decide if the preserved metal justified further processing. It can be speculated that different amounts of un-corroded metal were preserved in objects deposited at different times at the site over its long-term use, as suggested by finds of late-type objects at the site (section 2.1). The FFs may therefore represent the youngest and/or best preserved objects re-processed at the site.

The reason for not carrying from the site all FFs, despite the re-processing work performed on them, is not understood. It is possible that these fragments were abandoned as failures of processing or for a different reason. However, the presence of complete copper arrowheads within Horizon I (Fig. 2b), representing a readily available source of copper, may indirectly challenge the interpretation of FFs as failures.

The cause for mixing of re-processed ferrous pieces with fragmented copper slags in Horizon I is also open to interpretation. One possibility is the undertaking of metal processing operations elsewhere at the site, and then the dumping of all residues on top of undisturbed deposits of Horizon II and III as a way of marking the location of these undisturbed deposits in the mobile dune landscape, in order to find them in the future.

Finally, there is no archaeological evidence regarding hypothesised subsequent stages of the re-processing, i.e. places where the site's FFs were further processed into finished products. It is possible that Saruq al-Hadid was the first node in a regional network of iron recycling, in which the site's rich cache of ritually-deposited artefacts was effectively exploited as a metal mine, in order then to be transported to different locations for final fabrication.

The general timeframe for commencement of re-processing activities at Saruq al-Hadid is difficult to determine. At the Late Bronze/Early Iron Age site of 'Uqdat al-Bakrah in Oman, where a large number of scrap copper-base objects was discovered, recycling activities have been dated to the early Iron Age (Yule, 2018: 143; Gernez, 2018). At Saruq al-Hadid, the Late Pre-Islamic and early Islamic radiometric dates from stratigraphically-related metallurgical debris (Weeks et al., 2017) support a different reconstruction. It is likely that objects initially ritually deposited at Saruq al-Hadid were scavenged and re-processed centuries after deposition, possibly by people largely unaware of the complex activities and motives of this earlier society. The alternative possibility – that re-processing took place after only a short period of deposition, and by people who were familiar with preceding activities at the site – remains to be considered. The aggressive soils of Saruq al-Hadid can corrode iron objects after only a few years of burial, as seen from the finds of modern iron nails forgotten at the site for several years. The people who participated in and perhaps controlled activities at the site could have systematically re-processed the partly rusted objects, following any of a range of social, political, and/or economic considerations.

Overall, despite uncertainties, the combined archaeometric analyses presented here strongly support the hypothesis that complete iron artefacts from early Iron Age deposits at Saruq al-Hadid were subsequently re-processed, as summarised in Table 2.

6. Conclusions

The archaeometric investigation of ferrous fragments from Saruq al-Hadid indicates that operations incorporating the scavenging/retrieval, assessment, and re-processing of earlier deposited complete iron objects were a prominent component of human activities at the site, while the manufacture of new objects was unlikely to have taken place there at any time during its occupation. Underpinning this re-processing was a long-term tradition of ritual offerings and activities at the site, commencing in the early Iron Age, which led to the deposition of numerous iron artefacts. A substantial amount of the iron deposited in Horizons II and III appears to have been retrieved and re-processed through disassembly and forging, with c. 200 kg of residues from this processing being discarded in Horizon I.

Through a multivalent approach to the analysis and interpretation of metal processing operations, this study shows that heavily corroded iron objects – often disregarded for analysis due to their poor state of preservation and consequent challenges for interpretation – can provide unique insights into their complex working history. The investigation of such challenging remains requires an integrated research methodology incorporating spatial, morphological and archaeometric analyses, in order to illuminate the complicated biographies of deposition, corrosion, and re-processing. At Saruq al-Hadid, this research has provided an important new source of evidence for cultural activities undertaken at the site after its major period of occupation in the early Iron Age, and such an approach should prove applicable to other comparable archaeological assemblages.

Acknowledgments

This research project was funded by the Dubai Municipality (Contract 639/1/1413904) and the lead author is supported by a PhD studentship from the University of New England. We express our gratitude to Dubai Municipality and Dr Hussein Qandil for providing samples for the study and thank the infrastructure of the School of Environmental and Rural Sciences, UNE, for providing access to the X-Ray diffractometer used in the research. We also thank Hélène David-Cuny (Associate, Centre Français d'Archéologie et de Sciences Sociales Kuwait) for the photos of some of the analysed samples, and James Roberts (UNE) and Dr Steven Karacic (Florida State University) for their help and valuable comments in relation to the work undertaken. Finally, we thank two anonymous reviewers for valuable comments that significantly improved the study.

Appendix A. Supplementary data

Supplementary data to this article can be found online at https://doi.org/10.1016/j.jas.2018.11.003.

References

Benoist, A., 2007. An iron age II snake cult in the Oman peninsula: evidence from Bithnah (Emirate of Fujairah). Arabian Archaeol. Epigr. 18 (1), 34–54.
Boni, M., Maio, G., Frei, R., Villa, I.M., 2000. Lead isotopic evidence for a mixed provenance for Roman water pipes from Pompeii. Archaeometry 42 (1), 201–208.
Bradley, R., 1988. Hoarding, recycling and the consumption of prehistoric metalwork: technological change in western Europe. World Archaeol. 20 (2), 249–260.
Bray, P., Cuénod, A., Gosden, C., Hommel, P., Liu, R., Pollard, A.M., 2015. Form and flow: the 'karmic cycle'of copper. J. Archaeol. Sci. 56, 202–209.
Bray, P.J., Pollard, A.M., 2012. A new interpretative approach to the chemistry of copper-alloy objects: source, recycling and technology. Antiquity 86 (333), 853–867.
Brown, E.J., 1980. Traditional Blacksmiths and Metalworking in Kenya: an Ethno-archaeological Approach (unpublished D. Phil. thesis). University of Edinburgh.
Bouchar, M., Foy, E., Neff, D., Dillmann, P., 2013. The complex corrosion system of a medieval iron rebar from the Bourges' Cathedral. Characterization and reactivity studies. Corrosion Sci. 76, 361–372.
Contreras, R.F., Vila, B., Albarracín, P., Bukhash, R.M., Al Abbar, S.O., Radwan, M.B., Zein, H.M., 2017. Excavations in Area 2A at Sarūq al-Hadīd: iron Age II evidence of copper production and ceremonial activities. Proc. Semin. Arab. Stud. 47, 57–66.
Dungworth, D., 1997. Roman copper alloys: analysis of artefacts from northern Britain. J. Archaeol. Sci. 24 (10), 901–910.
Dungworth, D., Wilkes, R., 2007. An investigation of hammerscale. Hist. Metall. 43, 33–46.
Fell, V., 2004. Cremated: analysis of the metalwork from an iron age grave. In: Ashton, J., Hallam, D. (Eds.), Metal 04: Proc of the International Conference of Metal Conservation. National Museum of Australia, Canberra ACT, pp. 514–519.
Fleming, R., 2012. Recycling in Britain after the fall of Rome's metal economy. Past Present 217 (1), 3–45.
Gernez, G., 2018. Uqdat al-Bakrah in the context of eastern Arabia and the ancient near eastern archaeology. In: Yule, P., Gernez, G. (Eds.), Early Iron Age Metal-working Workshop in the Empty Quarter, Al-Zobira Province, Sultanate of Oman. Verlag Dr. Rudolf Habelt GmbH, Bonn, pp. 171–180.
Golfomitsou, S., Rehren, T., Eckmann, C., 2017. Conservation and archaeological science for the protection and understanding of ancient craftsmanship. In: Tsuneki, A., Yamada, S., Hisada, K. (Eds.), Cultural Heritage, Ancient West Asian Civilization. Springer, Singapore, pp. 199–217.
Gordon, R.B., Van Der Merwe, N.J., 1984. Metallographic study of iron artefacts from the eastern Transvaal, South Africa. Archaeometry 26 (1), 108–127.
Haerinck, E., Overlaet, B., 2004. The Iron Age III Graveyard at War Kabud. Chavar District, Pusht-i Kuh, Luristan, Luristan Excavation Documents. Acta Iranica, Leuven vol. V.
Herrmann, J.T., Casana, J., Qandil, H.S., 2012. A sequence of inland desert settlement in the Oman peninsula: 2008–2009 excavations at Saruq al-Hadid, Dubai, UAE. Arabian Archaeol. Epigr. 23 (1), 50–69.
Howari, F., Baghdady, A., Goodell, P., 2007. Mineralogical and gemorphological characterization of sand dunes in the eastern part of United Arab Emirates using orbital remote sensing integrated with field investigations. Geomorphology 83, 67–81.
Karacic, S., Boraik, M.R., Qandil, H.S., David-Cuny, H., 2017. Snake decorations on the Iron Age pottery from Saruq al-Hadid: a possible ritual centre? Proc. Semin. Arab. Stud. 47, 139–150.
Karageorghis, V., Kassianidou, V., 1999. Metalworking and recycling in late Bronze age Cyprus–the evidence from Kition. Oxf. J. Archaeol. 18 (2), 171–188.
Kubaschewski, O., 2013. Iron—binary Phase Diagrams. Springer Science & Business Media.
Kusimba, C.M., Killick, D.J., Cresswell, R.G., 1994. Indigenous and imported metals at Swahili sites on the coast of Kenya. Society. In: Childs, S.T. (Ed.), Culture, and Technology in Africa, 11. The University of Pennsylvania Museum, Philadelphia, pp. 63–77.
L'Héritier, M., Dillmann, P., Aumard, S., Fluzin, P., 2013. Iron? Which iron? Methodologies for metallographic and slag inclusion studies applied to ferrous reinforcements from Auxerre Cathedral. In: Humphris, J., Rehren, T. (Eds.), The World of Iron. Archetype Publications, London, pp. 409–420.
LaViolette, A.J., 2000. Ethno-archaeology in Jenné, Mali: craft and status among smiths, potters and masons. Cambridge Monographs in African Archaeology, vol. 49 Archaeopress, Oxford.
Levene, D., Ponting, M., 2015. Recycling economies, when efficient, are by their nature invisible. A first century Jewish recycling economy. In: Geller, M.J. (Ed.), The Archaeology and Material Culture of the Babylonian Talmud. Brill, Leiden, pp. 39–65.
Lombard, P., Kervran, M., 1989. Bahrain National Museum Archaeological Collections, Vol. 1. A Selection of Pre-islamic Antiquities from Excavations 1954-1975. Ministry of Information, Bahrain.
Magee, P., 1998. New evidence of the initial appearance of iron in southeastern Arabia. Arabian Archaeol. Epigr. 9 (1), 112–117.
Mangin, M., Fluzin, P., 2003. La petite sidérurgie en contexte rural: les forges du Haut-Auxois mandubien et de ses marges lingonnes (Côte-d'Or). Rev. Archeol. Picardie 1 (1), 141–156.
Marciuš, M., Ristić, M., Ivanda, M., Musić, S., 2012. Formation of iron oxides by surface oxidation of iron plate. Croat. Chem. Acta 85 (1), 117–124.
Millard, A.R., 1994. King solomon's shields. In: King, P.J., Coogan, M.D., Exum, J.C., Stager, L.E. (Eds.), Scripture and Other Artifacts: Essays on the Bible and Archaeology in Honor of Philip J. King. John Knox Press, Westminster, pp. 286.
Moorey, P.R., 1971. The loftus hoard of old Babylonian tools from tell sifr in Iraq. Iraq 33 (2), 61–86.
Moorey, P.R., 1994. Ancient Mesopotamian Materials and Industries: the Archaeological Evidence. Clarendon Press, Oxford.
Mouton, M., 2008. La Péninsule d'Oman de la fin de l'Âge du Fer au début de la période sassanide, 250 av.-350 ap. JC, Archaeopress. British Archaeological Reports, Oxford.
Muscarella, O., 1988. Bronze and Iron: Ancient Near Eastern Artifacts in the Metropolitan Museum of Art. Metropolitan Museum of Art, New York.
Neff, D., Dillmann, P., Bellot-Gurlet, L., Beranger, G., 2005. Corrosion of iron archaeological artefacts in soil: characterisation of the corrosion system. Corrosion Sci. 47 (2), 515–535.
Neff, D., Bellot-Gurlet, L., Dillmann, P., Reguer, S., Legrand, L., 2006. Raman imaging of ancient rust scales on archaeological iron artefacts for long-term atmospheric corrosion mechanisms study. J. Raman Spectrosc. 37, 1228–1237 An International Journal for Original Work in all Aspects of Raman Spectroscopy, Including Higher Order Processes, and also Brillouin and Rayleigh Scattering.
Neff, D., Vega, E., Dillmann, P., Bellot-Gurlet, L., Descostes, M., Béranger, G., 2007. Contribution of Iron Archaeological Artefacts to the Estimation of Average Corrosion Rates and the Long Term Corrosion Mechanisms of Low Carbon Steel Buried in Soil, Corrosion of Metallic Heritage Artefacts: Investigation, Conservation and Prediction for Long Term Behaviour. pp. 41–76.
O'Brien, P., 2016. The New Economic History of the Railways. Taylor Francis, United Kingdom.
Overlaet, B., 2003. The Early Iron Age in Pusht-i Kuh, Luristan, Luristan Excavation Documents IV. Peeters, Lovanii.
Pleiner, R., Bjorkman, J.K., 1974. The Assyrian iron age: the history of iron in the Assyrian civilization. Proc. Am. Phil. Soc. 118 (3), 283–313.
Pleiner, R., 1979. The technology of three Assyrian iron artifacts from Khorsabad. J. Near E. Stud. 38, 83–91.
Pole, L.M., 1982. Decline or survival? Iron production in West Africa from the seventeenth to the twentieth centuries. J. Afr. Hist. 23 (4), 503–513.
Potts, D.T., 1998. Some issues in the study of the pre-Islamic weaponry of southeastern Arabia. Arabian Archaeol. Epigr. 9 (2), 182–208.
Rehder, E., 1991. The decorated iron swords from Luristan: their material and manufacture. Iran 29, 13–19.
Roth, M.T. (Ed.), 2005. The Assyrian Dictionary: P. Oriental Institute, Chicago.
Samuels, L., 1980. Optical Microscopy of Carbon Steels. Asm Intl, Ohio.
Schwab, R., 2002. Evidence for carburized steel and quench-hardening in the'Celtic'oppidum of Manching. Hist. Metall. 36, 6–16.
Smith, C.S., 1971. The techniques of the Luristan smith. In: Brill, R.H. (Ed.), Science and Archaeology. MIT Press, Cambridge, MA, pp. 32–52.
Stepanov, I., Weeks, L., Salvemini, F., Al Ali, Y., Radwan, M., Zein, H., Grave, P., 2018a. Early Iron Age ferrous artefacts from southeastern Arabia: investigating fabrication techniques using neutron tomography, optical microscopy and SEM-EDS. Archaeol Archaeol Sci. https://doi.org/10.1007/s12520-018-0730-7.

Stepanov, I., Weeks, L., Salvemini, F., Al Ali, Y., Radwan, M., Zein, H., Grave, P., 2018b. Early Iron Age ferrous arte-facts from southeastern Arabia: investigating fabrication techniques using neutron tomography, optical mi-croscopy and SEM-EDS. Archaeol. Archaeol. Sci. https://doi.org/10.1007/s12520-018-0730-7.

Stepanov, I., Weeks, L., Franke, K., Overlaet, B., Magee, P., Alard, O., Cable, C., Al Ali, Y., Radwan, M.B., Zein, H., Grave, P., The provenance of iron age ferrous artefacts from south-eastern Arabia. In preparation.

Thornton, C., Pigott, V., 2011. Blade-type weaponry of Hasanlu period IVB. In: de Schauensee, M. (Ed.), Peoples and Crafts in Period IVB at Hasanlu, Iran, Hasanlu Special Studies IV. University of Pennsylvania Museum, Philadelphia, pp. 135–182.

Uqba, K.A., 1991. The Water Resources of the United Arab Emirates: a Comprehensive Empirical Appraisal of Their Status and Management (Unpublished D. Phil. Thesis). Durham University.

Van Der Merwe, N.J., Avery, D.H., 1982. Pathways to Steel: three different methods of making steel from iron were developed by ancient peoples of the Mediterranean, China, and Africa. Am. Sci. 70 (2), 146–155.

Weeks, L., Cable, C., Franke, K., Newton, C., Karacic, S., Roberts, J., Stepanov, I., David-Cuny, H., Price, D., Bukhash, R.M., Radwan, M.B., Zein, H., 2017. Recent archaeological research at Saruq al-Hadid, Dubai, UAE. Arabian Archaeol. Epigr. 28 (1), 31–60.

Weeks, L., Cable, C., Franke, K., Newton, C., Karacic, S., Roberts, J., Stepanov, I., David-Cuny, H., Price, D., Yousif Al Aali, Y., Radwan, M.B., Zein, H., 2018. Saruq al-Hadid: a persistent temporary place in late prehistoric Arabia. World Archaeol. 50.

Welton, A.J., 2016. Encounters with iron: an archaeometallurgical Reassessment of early Anglo-saxon spearheads and knives. Archaeol. J. 173 (2), 206–244.

Yule, P.A., 2016. Valorising the samad late iron age. Arabian Archaeol. Epigr. 27 (1), 31–71.

Yule, P., 2018. The finds. In: Yule, P., Gernez, G. (Eds.), Early Iron Age Metal-working Workshop in the Empty Quarter, Al-Zobira Province, Sultanate of Oman. Verlag Dr. Rudolf Habelt GmbH, Bonn, pp. 33–147.

Zettler, R.L., 1990. Metalworkers in the economy of Mesopotamia in the late third millennium BC. In: Miller, N.F. (Ed.), Economy and Settlement in the Near East: Analyses of Ancient Sites and Materials. University of Pensilvania Museum, Philadelphia, pp. 85–88.